Origin of ordered two-dimensional structure of Si(337)-4×1 transformed from Si(5 5 12)-2×1

Hidong Kim, Ganbat Duvjir, Otgonbayar Dugerjav, Huiting Li, and Jae M. Seo*
Department of Physics and Institute of Photonics and Information Technology, Chonbuk National University, Jeonju 561-756, Republic of Korea

(Received 31 March 2010; revised manuscript received 31 May 2010; published 18 June 2010)

Through combined studies using scanning tunneling microscopy (STM) and high-energy-resolution synchrotron photoemission, the origin of irreversible structural transformation from Si(5 5 12)-2×1 to Si(337)-4×1 with (113) facets has been investigated. From the C-dosed Si(5 5 12) surface, it has been found by STM that the transformation from (5 5 12) to (337) starts from a tetramer (T) row and a π-bonded (π) chain in the (5 5 12) surface, and simultaneously the rest part of (5 5 12) converts to T rows and π chains, which will be transformed to (337) with additional Si atoms. By Si 2*p* and C 1*s* core-level photoemission studies using synchrotron radiation on the identical system, it has been confirmed that such an irreversible structural transformation is due to subsurface C atoms. If the (337) terrace is only composed of T rows and π chains with a 2× periodicity, the compressive stress exists so that the (337) terrace becomes unstable. However, subsurface C atoms release this compressive stress through breaking one-dimensional structures and induce a stable surface composed of 4×1 dotlike structures with additional Si atoms.

DOI: 10.1103/PhysRevB.81.245422 PACS number(s): 68.35.B−, 68.37.Ef, 79.60.−i

I. INTRODUCTION

Among stable high-index Si surfaces between (001) and (111) planes, the reconstructed Si(5 5 12)-2×1 is known to have planar, single-domain, and one-dimensional (1D) structures with a long periodicity of 5.35 nm perpendicular to the $[1\bar{1}0]$ direction.[1,2] So, Si(5 5 12)-2×1 is expected to be used as a template for the growth of 1D nanostructure[1,3–11] and high-quality heteroepitaxial films.[12] A big obstacle, however, is in its instability that the Si(5 5 12)-2×1 is easily faceted to (7 7 17), (337), (113), (112), (335), (225), (5 5 11), (7 7 15), etc. by deposited materials[3–11,13] or by external stress.[14] On the other hand, under a specific condition of flashing the Si(5 5 12) surface to remove native-oxide layer during clean surface preparation, the surface is often faceted to (337) and (113), and the (337) is reconstructed to a two-dimensionally (2D) ordered 4×1 structure. Interestingly, such an irreversible structural transformation is not always detected. Once the surface is transformed to (337)-4×1, it becomes very stable. Similar phenomena induced just by thermal treatment during preparation of the reconstructed surfaces have also been reported in the transformation from Si(001)-2×1 to Si(001)-*c*(4×4) as well as from Si(114)-2×1: A phase [composed of dimer (D), rebonded-atom (R), and tetramer (T) rows] to Si(114)-2×1: B phase (composed of D-T-T rows).[15,16] Up to now, the origin of such irreversible structural transformation is thought to be due to stress induced by subsurface C impurity, which is confirmed by direct carbon detection[17,18] or by induced reconstruction transformation by intentional C injection using graphite,[19,20] SiC,[21,22] or C_2H_2/C_2H_4.[15,23–28]

In the present study, using scanning tunneling microscopy (STM) and high-resolution synchrotron photoemission spectroscopy experiments, the origin of such structural transformation from 1D Si(5 5 12)-2×1 to 2D Si(337)-4×1 has been investigated by dosing C_2H_2 gas as well as Si evaporation on the clean Si(5 5 12)-2×1.

II. EXPERIMENTAL

A Si(5 5 12) substrate of size 13×3×0.3 mm^3 was cut from an *n*-type (P-doped) wafer and degreased with organic solvents in air. It was mounted on a molybdenum sample holder and introduced in an ultrahigh vacuum (UHV) chamber of a base pressure 2×10^{-10} Torr. Then it was outgassed at 700 °C for 12 h. After outgassing, the substrate was flashed at about 1150 °C by resistive heating to remove the native-oxide layer. Each flashing period was kept below three seconds for preventing the pressure from soaring over 3×10^{-10} Torr and the accumulated flashing period was about 5 min. When flashing was completed, the surface was reconstructed by slow cooling from 900 °C to room temperature (RT) at a rate of 1° s^{-1}. Finally, to remove intrinsic C impurities, the sample was oxidized with 1×10^{-6} Torr O_2 at 650 °C and flashed about 1150 °C. As an external C source, C_2H_2 gas was dosed on the Si(5 5 12) surface held at 650 °C. The amount of the dosed C_2H_2 molecules was controlled by varying the exposure period at 1×10^{-6} Torr. After C_2H_2 exposure, the sample was additionally annealed at 750 °C for 3 min in order to thermally dissociate C_2H_2 and incorporate C into Si(5 5 12).[29] Then, the substrate was flashed at 1150 °C for 3 min to remove remaining clusters on the substrate and cooled down from 900 °C to RT at a rate of 1° s^{-1}.

Error-signal STM images were acquired in the constant-current mode ($I_{tunneling}$=0.5 nA) at RT. They are obtained by recording the difference between the set current and the measured current controlling the *z*-axis motion in the feedback mode in order to single out the intensity variation.[30] The Si 2*p* and C 1*s* core levels were obtained at the 8A2 undulator beam line of Pohang Accelerator Laboratory in Korea using a high-resolution electron analyzer, Scienta 3000, at RT.

III. RESULTS AND DISCUSSION

Figure 1(a) shows a topographic STM image of the Si(5 5 12) surface obtained by flashing at 1150 °C for 5 min

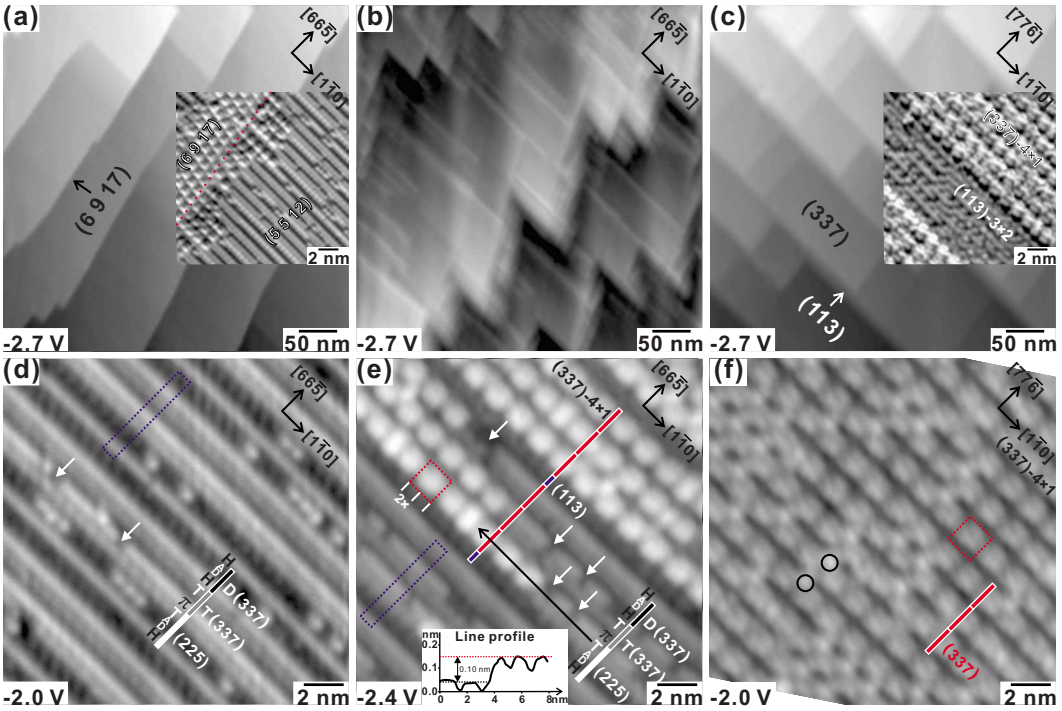

FIG. 1. (Color online) [(a)–(c)] Filled-state topography STM images showing structural transformation from Si(5 5 12)-2×1 to Si(337)-4×1 induced by flashing only at 1150 °C. [(d)–(f)] Magnified images of (a)–(c), respectively. (a) Initial (5 5 12) terraces with (6 9 17) facets. The inset error-signal image shows a boundary between a (6 9 17) facet and a (5 5 12) terrace. (b) The image in a transitional period from (5 5 12) to (337), obtained after annealing at 1150 °C for 3 min. White lines on (5 5 12) terraces grow from the (6 9 17) facets. (c) Fully converted (337) terraces having (113) facets, obtained after annealing at 1150 °C for 6 min. The inset error-signal STM image shows a Si(113)-3×2 between two (337) terraces. (d) One period of Si(5 5 12)-2×1 terrace consists of a (225) subunit and two (337) subunits. Four kinds of 1D structures of H chains, π chains, D-A rows, and T rows are shown. (e) White lines in (b) consist of (337)-4×1. A line profile along the black arrow is shown in the inset. Blue (dark gray) and red (gray) rectangles designate unit cells of (5 5 12)-2×1 and (337)-4×1, respectively. (f) Terrace of (337)-4×1. Additional features are marked by circles.

followed by slow cooling for reconstruction. It shows Si(5 5 12) terraces having both (6 9 17) and (113) facets.[31] In the inset of Fig. 1(a), one part of the boundary between a (6 9 17) facet and a (5 5 12) terrace is magnified. At the lower terrace of Si(5 5 12), it can be found that 1D features start to grow from the (6 9 17) facet toward the (5 5 12) terrace. After additional flashing for 3 min followed by slow cooling for reconstruction, the straight (6 9 17) facet has been changed to a saw-toothlike facet, as shown in Fig. 1(b). White lines along the $[1\bar{1}0]$ direction reach at the (6 9 17) facets in the upper terrace of (5 5 12). After additional 3-min flashing the sample shown in Fig. 1(b) and reconstruction, the whole terrace is finally converted to a *new* plane composed of Si(113)-3×2 facets parallel to the $[1\bar{1}0]$ direction, instead of (6 9 17) facets, and (337) terraces as shown in Fig. 1(c).[32] One of these (113) facets is shown in the inset of Fig. 1(c). It can be found that the (5 5 12) terrace is fully covered with these 1D features.

In order to analyze these conversions shown in Figs. 1(a)–1(c), their magnified topographic images of terraces are shown in Figs. 1(d)–1(f), respectively. Figure 1(d) shows one Si(5 5 12)-2×1 unit [The blue (dark gray) rectangle represents a unit cell of Si(5 5 12)-2×1] is composed of one (225) [more precisely, (4 4 10); unless all of three indices are odd numbers, the indices should be multiplied by two] subunit and two (337) subunits. One period along the $[66\bar{5}]$ direction of bulk terminated (337) can be considered as one (112) [more precisely, (224)] and one (113). One (112) is reconstructed to either a π-bonded (π) chain or a honeycomb (H) chain, and one (113) to either a tetramer (T) row or a dimer-adatom (D-A) row. One (337) subunit with a tetramer row [T(337)] is composed of a π and a T; the other (337) with a dimer-adatom row [D(337)] is composed of an H and a D-A; and the remaining (225) subunit can be considered as one (337) plus one (113) and is reconstructed to a D(337) and a T row.[33] Broken 1D defects, shown only in the π chain (marked by white arrows), are indicators to distinguish the π chain from the H chain, as shown in Fig. 1(d). Figure 1(e), a magnified image of Fig. 1(b), shows how the new line feature evolves from Si(5 5 12)-2×1. Comparing it with the remaining Si(5 5 12)-2×1, a row (T or D-A) and a chain (π or H) become a dotlike row, which means the basic period perpendicular to the $[1\bar{1}0]$ direction is 1.57 nm that of a (337) unit. And its period along the $[1\bar{1}0]$ direction is 4× twice that of the D-A row, as marked by small white bars and letters "2×." As a result, the new dotlike structures are deduced to be (337)-4×1 and its unit cell is designated by one rectangle whose size is 1.54 nm ×1.57 nm. Since one (5 5 12) unit corresponds three (337) units and one (113), as marked by red (gray) and blue (dark gray) bars, every three (337)'s should have one (113) as surplus. We can see broken 1D defects (marked by white arrows) on all chains like those

found on the π chain in Fig. 1(d). In addition, from the line profile following the black arrow in Fig. 1(e), it can be found that the height of dotlike (337)-4×1 is larger than that of the original (5 5 12)-2×1 by about 0.1 nm, which means that it needs additional Si atoms. These Si atoms are thought to be supplied from dissolved (6 9 17) facets. In fact, looking carefully at the inset in Fig. 1(a), dotlike features start from the (6 9 17) facet and expand for themselves at the lower terrace of (5 5 12) up to the end of the terrace as shown in Fig. 1(b). The boundary between the facet and the terrace is drawn with a red (gray)-dotted line in the inset of Fig. 1(a). The dotlike feature in (6 9 17) facets had already been reported as a unit cell composed of four (337) unit cells along the $[1\bar{1}0]$ direction with a $3\times(011)$ step.[31] In Fig. 1(f), the fully transformed (337)-4×1 is shown. Residual (113) steps in Fig. 1(e) were bunched to (113)-3×2 facets, as shown in Fig. 1(c).

Once the whole surface structure is converted to Si(337)-4×1, the (5 5 12)-2×1 surface cannot be recovered only by flashing at elevated temperatures, which indicates that this Si(337)-4×1 is thermally stable. After oxidizing Si(337)-4×1 under 600 L of O_2 exposure (that is, 10^{-6} Torr O_2 for 10 min) and flashing it at 1150 °C for 3 min, it is found that this Si(337)-4×1 partially returns to Si(5 5 12)-2×1. Repeating this process, the original Si(5 5 12)-2×1 has been gradually recovered in the reverse order, that is, from the surface like Fig. 1(c) to that like Fig. 1(a). After about 10 000 L of O_2 exposure and flashing, any dotlike structure has not been detected even near (6 9 17) facets. Once (5 5 12)-2×1 is recovered in this way, it would not be transformed to (337)-4×1 by annealing at elevated temperatures. Such experimental evidences imply that subsurface impurities are closely related to conversion of Si(5 5 12)-2×1 to Si(337)-4×1.

As mentioned earlier, from the magnified image of a (6 9 17) facet shown in the inset of Fig. 1(a), the dotlike structure starts growing from the (6 9 17) facet at the lower terrace of (5 5 12). In order to confirm that this dotlike (337)-4×1 structure needs additional Si atoms, 0.01 nm of Si were deposited on the sample held at 500 °C. A filled-state STM image (error signal) and an empty-state STM image (error signal) of the same area [enclosed by blue (dark gray) rectangles] on this surface are shown in Figs. 2(a) and 2(b), respectively. The (337)-4×1 rows shown in the middle of a terrace deserve special mention. In the case of Fig. 1(b), these dotlike structures grow from (6 9 17) steps. In addition, they are different from either π/H chains or T/D-A rows formed on the clean Si(5 5 12)-2×1 surface in homoepitaxy at 500 °C or 550 °C.[34,35] In the empty-state image of the present bias condition, two kinds of chains and rows are clearly distinguished: π chains look smoother than H chains with distinct 1× features and have defects marked with white arrows; T rows have clearer dark lines in the middle along the $[1\bar{1}0]$ direction than D-A rows which can host addimers. These images imply that the transformation from (5 5 12)-2×1 to (337)-4×1 starts always from the T row in a (225) and the π chain in the nearest T(337), as marked by numbers "1's." For this transformation, the inset in Fig. 2(a), the corresponding topographic image, says that additional Si

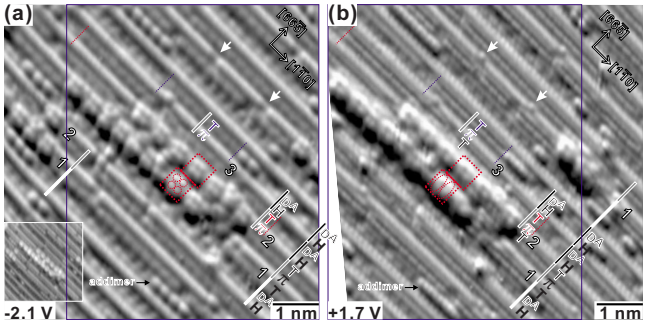

FIG. 2. (Color online) STM images (error signal) of the Si(5 5 12) surface having both (5 5 12)-2×1 and (337)-4×1, obtained after 0.01 nm of Si deposition on the sample. (a) Filled-state image. (b) Empty-state image. Blue (dark gray) rectangles in (a) and (b) designate the same area. The inset in (a) is the corresponding topographic image. Red (gray)-dotted rectangles in (a) and (b) represent two unit cells of (337)-4×1. T: tetramer row, π: π-bonded chain, D-A: dimer-adatom row, and H: honeycomb chain.

atoms are needed, in that the (337)-4×1 area is higher than the (5 5 12)-2×1 area. Then, the neighboring D(337) (=H+D-A) is converted to a T(337) (=π+T) as shown in the section designated by two red (gray)-dotted bars in Figs. 2(a) and 2(b), which means that the previously formed (337)-4×1 row is under tensile strain and applies compressive stress to the neighboring D(337) along the $[66\bar{5}]$ direction.[33] This just changed π together with the T row in the T(337) is transformed to a new (337)-4×1 row, as marked by numbers "2's." This causes the H chain and the D-A row in the nearest neighbor to be changed to a π chain and a T row [in the section designated by two blue (dark gray)-dotted bars and marked by numbers "3's." in Figs. 2(a) and 2(b)], which will be transformed into a (337)-4×1 row with additional Si atoms. In this way, (337)-4×1 is expanded to the $[66\bar{5}]$ direction. Such expansion mechanism of the (337)-4×1 row is confirmed by the fact that the (337)-4×1 row formed at the T row in the (225) and the π chain in the T(337) of Si(5 5 12)-2×1 is longer than the others. A unit cell marked by red (gray)-dotted rectangles appears such as four protrusions in the filled-state image and two ovals in the empty-state image. In addition, these STM images show that the precursor of a (337)-4×1 row is a T row and a π chain. Defects appearing on the chains, marked with white arrows, also suggest that transformation from H chain to π chain is needed for making (337)-4×1 since such defects are not detected from H chains on Si(5 5 12)-2×1.

It has been reported that the clean Si(337) surface is unstable and it facets into Si(5 5 12) and Si(111).[36–38] Especially, the Si(337) surface composed of only T(337) is unstable since it is under strong compressive strain.[36] On the other hand, for the case of Si(5 5 12), one (225) [=H+D-A+T], one compressive T(337) [=π+T], and one tensile D(337) [=H+D-A] subunits in one period of Si(5 5 12)-2×1 are under stress balance for themselves so the Si(5 5 12) surface becomes stable.[33] Narrow Si(337) terraces are composed of D(337)'s along with one (225) and one T(337).[2] So, for stability of wide (337) terrace, it needs another kind of atom which can induce stress balance. Similar to this, novel

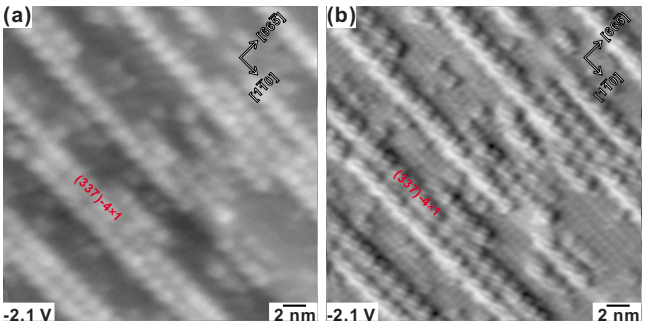

FIG. 3. (Color online) (a) Topographic and (b) error-signal filled-state STM images showing structural transformation from Si(5 5 12)-2×1 to Si(337)-4×1, obtained after exposing 120 L of C_2H_2 at 650 °C and postannealing at 750 °C for 3 min. About half of the surface area is converted to (337)-4×1.

reconstructions induced by specific-heat treatments under UHV have also been reported for Si(001) and Si(114).[15,18] In these cases, C-containing molecules in the residual gases such as CO, CO_2, and hydrocarbons are thought to be adsorbed on the surface and decomposed by flashing. Therefore, the subsurface carbon atom is thought to be the origin of such other kinds of reconstructions, for Si(001), Si(111), and Si(114).[15,23,39]

In order to confirm whether subsurface C also induces the present Si(337)-4×1 or not, Si(5 5 12)-2×1 has been exposed to C_2H_2 gas. Prior to C_2H_2 exposure, it has been checked that the (5 5 12) terraces adjacent to (6 9 17) facets do not have any trace of the dotlike structure of (337)-4×1. The pre-existing dotlike structures had been cleared by repeated oxidation and flashing. Then, the Si(5 5 12)-2×1 surface was exposed to 120 L of C_2H_2 at 650 °C and postannealed at 750 °C for 3 min, which causes thermal dissociation of C_2H_2 and C incorporation into Si(5 5 12). In Fig. 3(a), a filled-state topographic STM image and in Fig. 3(b), the corresponding error-signal image of the C-dosed (5 5 12) surface are shown. It has been estimated that about half of the surface has been transformed to (337)-4×1. From the topographic image Fig. 3(a), the (337)-4×1 area turns out to be higher than the other area. In Fig. 3(b), giving more information on detailed structures, the structure of the bottom area turns out to be different from that of the original Si(5 5 12)-2×1. This indicates that Si atoms were rearranged at the terrace to form the (337)-4×1 structure. From these images, it has been confirmed that subsurface C also induces the (337)-4×1 structure, which needs additional Si atoms. One of the distinguished difference between Fig. 1 and Fig. 3 is in the place where the growth seed is located. That is, for the case of Fig. 1, the additional Si atoms are supplied from (6 9 17) facets, while for the case of Fig. 3, the additional atoms are supplied from the terrace.

Based on the information from Figs. 1–3, we built an atomic structural model of Si(337)-4×1, as shown in Fig. 4(c). The unit cells of Si(337)-4×1 are marked by red (gray)-dotted rectangles in Fig. 4(a). There also exist a number of irregularities having a spacing of 1× or 2× as marked with "1×" and "2×." A magnified image showing a detailed

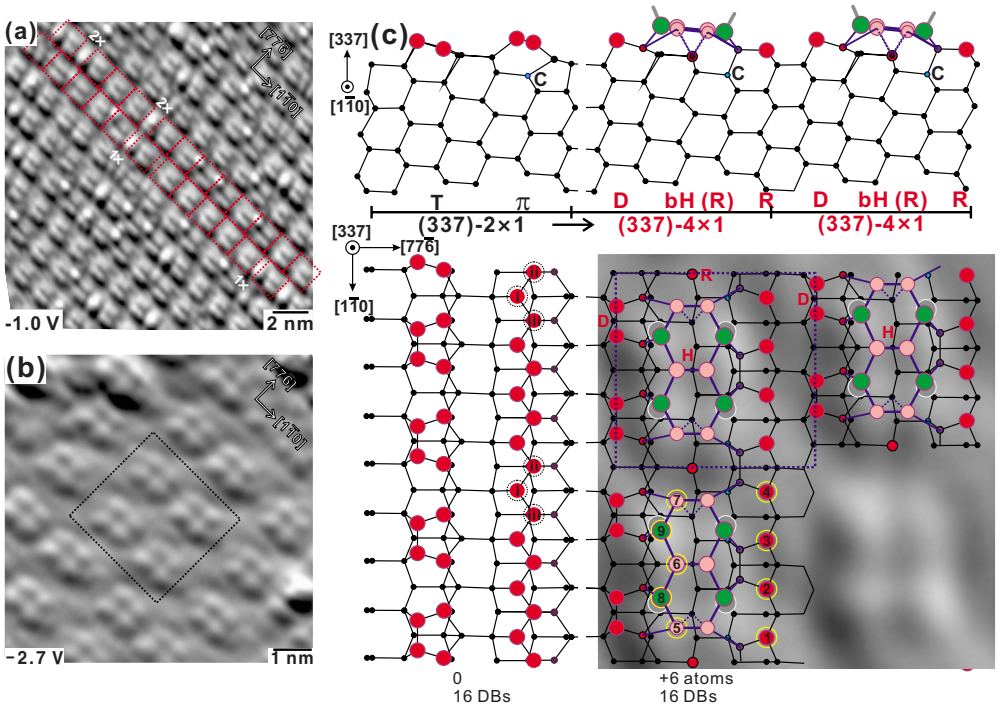

FIG. 4. (Color online) STM images and corresponding structural model of Si(337)-4×1. (a) Filled-state error-signal image of Si(337)-4×1 showing a large area of a well-ordered terrace. I_t: 0.5 nA, V_s: −1.0 V, and scan area: 17 nm×17 nm. (b) Magnified image of Si(337)-4×1 showing a detailed structure. I_t: 0.5 nA, V_s: −2.7 V, and scan area: 8 nm×8 nm. (c) Side- and top-view structural models of Si(337)-4×1. Left 1/3, a precursor, Si(337)-2×1 composed of a T row and a π chain, is inserted for comparison. The image of the area outlined by a dotted rectangle in (b) is magnified and overlapped on the top-view model. T: tetramer row, π: π-bonded chain, D: dimer row, bH: broken honeycomb chain, and R: rest atom.

structure of the Si(337)-4×1 unit cell is shown in Fig. 4(b). In this figure, four protrusions per unit cell are remarkable. In Fig. 4(c), the side- and top-view models are shown. For comparison, the precursor structure of Si(337)-4×1 composed of a T row and a π chain are displayed on the left side. On the right side, the final structural model of Si(337)-4×1 are overlapped on the magnified image of Fig. 4(b). These two structures are thought to be induced by subsurface C atoms [remarked with small blue (dark gray) circles in the top panel of Fig. 1(c)] whose size is smaller than that of Si. They are unstable especially due to a five-member ring in the π chain in the precursor state. In here, the compressive stress is created by the just formed neighboring (337)-4×1 row, as shown in Fig. 2. However, a large (337) terrace composed of only T rows and π chains, especially induced by subsurface C could not be sustained, unless the change in reconstruction through introducing additional Si atoms from either (6 9 17) facets or by Si deposition. The first step to release this compressive stress is breaking the π chain, as marked with white arrows in Fig. 1(e), releasing stress parallel to the $[1\bar{1}0]$ direction. At this time, atoms marked with roman numerals "i–iii" in Fig. 4(c) are removed per 4× along the $[1\bar{1}0]$ direction, leaving a rest atom behind per 4× periodicity, as shown in the right and bottom panel of Fig. 4(c). As the second step, for releasing compressive stress perpendicular to the $[1\bar{1}0]$ direction, four Si atoms per (337)-4×1 unit cell are inserted into the five-member ring as rest atoms as marked with arabian numerals "1–4" in Fig. 4(c) to relax compressive strain perpendicular to the $[1\bar{1}0]$ direction. At this time, the dimer parts of T rows remain as D's. In addition, five Si atoms per (337)-4×1 unit cell are inserted between the T row and the π chain as marked with arabian numerals "5–9" in Fig. 4(c) per unit cell, forming an H chain, which is broken by a 4× period. As a result, all the strain induced by subsurface C is relaxed and a stable (337)-4×1 surface is obtained. In here, the direction of the dangling bonds in the broken H chain are designated by green bars on green circles in the side view model of Fig. 4(c). Four protrusions of the magnified image overlapped on the top-view model of (337)-4×1 match well with the green big circles considering the direction of the dangling bonds.

In order to confirm the effect of carbon, the carbon-dosed surface was studied by the photoemission spectroscopy at the synchrotron radiation facility. In Fig. 5, C 1*s* core-level spectra obtained from the C-doped Si(5 5 12) surface are shown. The spectra were curve fitted by a standard least-squares fitting procedure using Voigt functions with Lorentzian and Gaussian widths of 0.15 eV and 0.65 eV, respectively. The clean Si(5 5 12)-2×1 surface did not show any C-related feature. On the other hand, a distinct C 1*s* core level was detected from the C-dosed surface (i.e., 400 L of C_2H_2 exposure at 650 °C and postannealing at 750 °C for 3 min) as shown in Fig. 5(a). From this surface, a major species, C_M, at the binding energy of 282.8 eV and two minor species, C_H at 283.4 eV and C_L at 282.0 eV were identified. After flashing it at 1150 °C additionally, three species, C_{MF} at 282.9 eV, C_{HF} at 283.5 eV, and C_{LF} at 282.1 eV were detected as shown in Fig. 5(b). Comparing these two spectra, all three peaks shifted to higher binding energy by 0.1 eV, and intensities of C_M and C_H decreased to about 1/2 of the original one. Their behaviors are similar to those of the Si_nC-related C 1*s* species in the C-dosed Si(114)-2×1 after flashing at an elevated temperature.[15] This means that peaks C_M and C_H in Fig. 5(a) are related to surface Si_nC structures. Through additional flashing at 1150 °C, more C atoms occupied subsurface C-Si_4 sites, which was manifested by C_{MF} in Fig. 5(b).[29,40] The high-binding-energy species, C_{HF} is related to partially decomposed CH_x species adsorbed from the residual gases or atomic C species with unsaturated bond(s) on the surface.[29] This result also confirms that the structural transformation is due to subsurface C atoms. Even though the solubility of C atoms in bulk Si is very low (less than 10^{-3}%) due to the large difference in their atomic sizes,[39] there were some reports that the subsurface solubility can be enhanced up to tens of percent through using nonequilibrium methods such as thermal dissociation of C_2H_2 at 650° on the Si surface, and that the structure of reconstructed surfaces is changed by subsurface C atoms.[23]

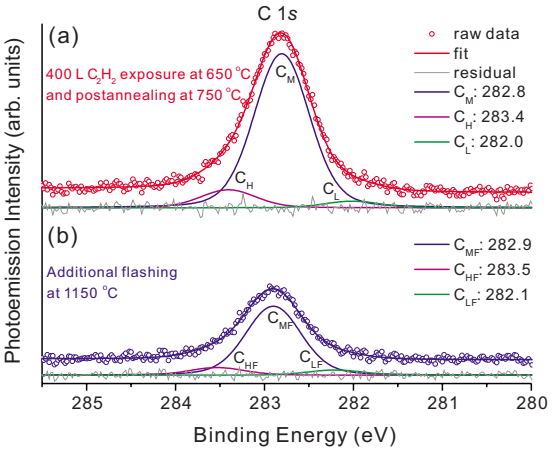

FIG. 5. (Color online) C 1*s* core-level photoemission spectra of Si(337)-4×1, obtained with 353 eV photon at normal-emission angle and its fitting ($\gamma_{Lorentzian}$=0.15 eV and $\sigma_{Gaussian}$=0.65 eV). (a) From the surface exposed to 400 L of C_2H_2 at 650 °C and postannealed at 750 °C for 3 min. (b) From the Si(337)-4×1 surface, obtained after additional flashing at 1150 °C for 3 min.

In order to observe the binding-energy shift of Si 2*p* due to C atoms, the corresponding Si 2*p* core-level spectra obtained at normal emission are shown in Fig. 6. The raw data designated by circles were analyzed by a standard least-squares fitting procedure using Voigt functions with Lorentzian width of 0.10 eV and Gaussian width of 0.35 eV for the bulk species (Gaussian widths of 0.39 eV, 0.55 eV, and 0.48 eV for S1, S2, and S, respectively), after subtracting the Shirley-type background.[41] The branching ratio was 0.43 and the spin-orbit splitting energy was 0.6 eV. The corresponding fitting result was listed in Table I. In Fig. 6(a), two kinds of surface-related peaks, S1 and S2, and the bulk peak B consist of the spectra of the clean Si(5 5 12)-2×1 surface. The surface core-level shifts (SCLSs or binding-energy shift), S1 and S2, relative to the bulk peak are +0.21 eV and −0.50 eV, respectively. Such shifts are due to charge transfer from downward atoms to upward atoms of π/H chains and T/D-A rows. As a result of charge transfer, the surface orbit-

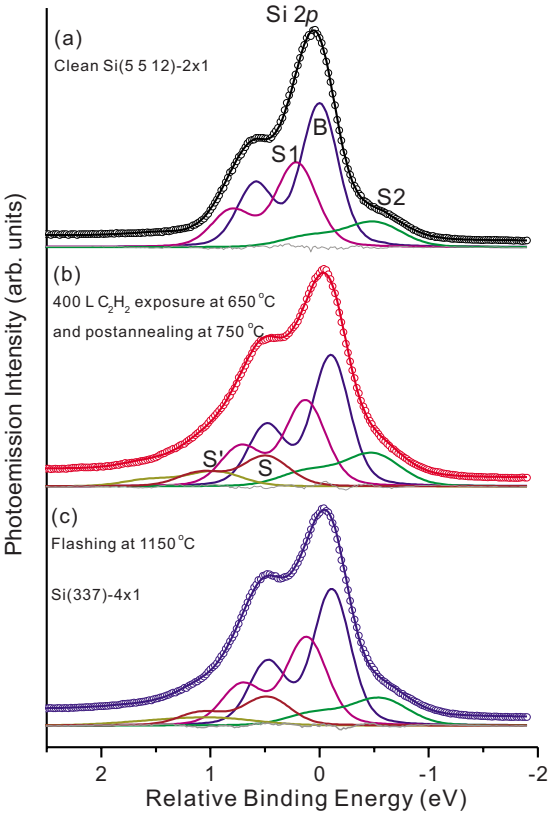

FIG. 6. (Color online) Si 2*p* core-level photoemission spectra of Si(5 5 12)-2×1 and Si(337)-4×1, obtained with 130 eV photon at normal-emission angle and their curve fittings. (a) Clean Si(5 5 12)-2×1 surface. (b) Exposed to 400 L of C_2H_2 at 650 °C and postannealed at 750 °C for 3 min. (c) Si(337)-4×1 surface, obtained after additional flashing at 1150 °C for 3 min. Detailed fitting results are listed in Table I.

als are rehybridized from sp^3 toward an sp^2-like and s^2p^3-like configurations for the downward and upward atoms.[42] The high-binding (low-binding) energy species, peak S1 (S2), corresponds to downward (upward) atoms of π/H chains and T/D-A rows. The resulting intensity ratio of S1 to S2 is 2.6. Though the numbers of upward and downward atoms are almost the same in the clean Si(5 5 12)-2×1,[33] part of the subsurface atoms bonded to π/H chains and T/D-A rows contribute to the high-binding species, S1 so that the intensity of S1 seems to be larger than that of S2 in Fig. 6(b).[43]

When C atoms are dosed on Si(5 5 12)-2×1 through exposing the surface at 650 °C to 400 L of C_2H_2 and postannealing at 750 °C for 3 min, two additional high-binding-energy species, S and S′ appear, as shown in Fig. 6(b). Their SCLS's relative to the bulk one are +0.60 eV and +1.06 eV, respectively. On the other hand, the bulk peak shifts to lower binding energy by 0.1 eV. Since the wafer is *n* type, this implies that such treatment induced more band bending by 0.1 eV. Such an additional band bending is induced by gap states originating from surface defectlike Si_nC clusters,[22] and the structural change from Si(5 5 12)-2×1 to phase Si(337)-4×1.

After flashing at 1150 °C, as shown in Fig. 6(c) and listed in Table I, the bulk binding energy shifts back by 0.01 eV, which means that the density of the interfacial states is negligibly changed. In here we can find that two additional surface-related peaks, S and S′, whose SCLS's are +0.59 eV and +1.06 eV, respectively, are still remaining but their intensities were reduced by flashing due to decrease in surface Si_nC. Since the electronegativity of C (2.55) is larger than that of Si (1.90), charges tend to transfer from Si to C.[44] From the large relative binding energy of S′ (i.e., +1.06 eV relative to the bulk), it can be deduced that this species is due to SiC localized at the surface.[41] On the other hand, peak S, with the relative binding energies around +0.59 eV, arises from interfacial Si atoms directly bonded to subsurface C atoms (i.e., C-Si_4 sites).[15] Such binding-energy shifts were also reported in either Si(001)-*c*(4×4) or Si(114)-2×1: D-T-T,[15,23,39] where C atoms occupy the subsurface site such as in Fig. 4(c).

IV. CONCLUSION

Through C incorporation using C_2H_2 as a C source, the well-ordered two-dimensional Si(337)-4×1 having subsurface C atoms has been generated from the clean Si(5 5 12)-2×1. As a precursor stage of such structural transformation, all the 1D structures of Si(5 5 12)-2×1 have been changed to π chains and T rows by substitutionally incorporated C atoms. Due to C atoms inducing compressive strain on the surface, π chains are preferentially broken. Additionally Si atoms are inserted into the five-member ring

TABLE I. Fitting results of SCLS's or binding-energy shift and relative intensities (RI) to that of the bulk for the Si 2*p* spectra shown in Fig. 6. The SCLS's are referred to the bulk peak (B) in kinetic energy (KE). Branching ratio: 0.43, spin-orbit splitting energy: 0.6 eV, and Lorentzian width: 0.10 eV are commonly used.

		Figure 6(a)		Figure 6(b)		Figure 6(c)	
Species	Gaussian width (eV)	SCLS (eV)	RI	SCLS (eV)	RI	SCLS (eV)	RI
B (KE)	0.35	28.10	1	28.20	1	28.21	1
S1	0.39	+0.21	0.64	+0.23	0.72	+0.23	0.71
S2	0.55	−0.50	0.25	−0.38	0.36	−0.44	0.29
S	0.48			+0.60	0.29	+0.59	0.26
S′	0.53			+1.06	0.16	+1.06	0.11

and between the T row and the π chain to relax the compressive stress. So the resulting atomic structure turns out to be composed of broken H chains, dimers, and rest atoms. The newly reconstructed (337) terrace is not faceted further by extended annealing at elevated temperatures, which implies that the instability of the Si(5 5 12) surface can be overcome by proper C incorporation and additional Si atoms. Homogeneity and stability of this new phase indicate its potential as a template for fabrication of 2D nanostructure or a substrate for epitaxial growth of optoelectronic devices. Through the present C-incorporation study, it has been confirmed that C atoms, having extremely low solubility in bulk Si, have also stable substitutional sites at the subsurface of the high-index Si surface.

ACKNOWLEDGMENTS

For conducting the present work, H.K. was supported by the Korea Research Foundation Grant funded by the Korean Government (Grant No. KRF-2008-359-C00016). This work was also supported by the Korea Research Foundation Grant funded by the Korean Government (Grant No. KRF-2008-521-C00082).

*seojm@jbnu.ac.kr; http://nano.chonbuk.ac.kr

[1] A. A. Baski, S. C. Erwin, and L. J. Whitman, Science **269**, 1556 (1995).
[2] A. A. Baski, S. C. Erwin, and L. J. Whitman, Surf. Sci. **392**, 69 (1997).
[3] S. R. Blankenship, H. H. Song, A. A. Baski, and J. A. Carlisle, J. Vac. Sci. Technol. A **17**, 1615 (1999); H. H. Song, K. M. Jones, and A. A. Baski, *ibid.* **17**, 1696 (1999); K. M. Jones, H. H. Song, and A. A. Baski, J. Clust. Science **10**, 573 (1999); A. A. Baski, K. M. Jones, and K. M. Saoud, Ultramicroscopy **86**, 23 (2001); A. A. Baski and K. M. Saoud, J. Clust. Science **12**, 527 (2001); A. A. Baski, K. M. Saoud, and K. M. Jones, Appl. Surf. Sci. **182**, 216 (2001); J. W. Dickinson, J. C. Moore, and A. A. Baski, Surf. Sci. **561**, 193 (2004).
[4] Y. Peng, H. Minoda, Y. Tanishiro, and K. Yagi, Surf. Sci. **493**, 508 (2001).
[5] S. S. Lee, N. D. Kim, C. G. Hwang, H. J. Song, and J. W. Chung, Phys. Rev. B **66**, 115317 (2002).
[6] J. R. Ahn, Y. J. Kim, H. S. Lee, C. C. Hwang, B. S. Kim, and H. W. Yeom, Phys. Rev. B **66**, 153403 (2002); J. R. Ahn, W. H. Choi, Y. K. Kim, H. S. Lee, and H. W. Yeom, *ibid.* **68**, 165314 (2003); J. R. Ahn, H. W. Yeom, E. S. Cho, and C. Y. Park, *ibid.* **69**, 233311 (2004).
[7] S. Cho and J. M. Seo, Surf. Sci. **565**, 14 (2004).
[8] M. Kumar, V. K. Paliwal, A. G. Joshi, Govind, and S. M. Shivaprasad, Surf. Sci. **596**, 206 (2005); M. Kumar, Govind, V. K. Paliwal, A. G. Vedeshwar, and S. M. Shivaprasad, *ibid.* **600**, 2745 (2006).
[9] H. Li, Y.-N. Xu, Y.-Z. Zhu, H. Kim, and J. M. Seo, Phys. Rev. B **75**, 235442 (2007).
[10] J. Liu, M. Takeguchi, H. Yasuda, and K. Furuya, J. Cryst. Growth **237-239**, 188 (2002).
[11] S. Jeong, H. Jeong, S. Cho, and J. M. Seo, Surf. Sci. **557**, 183 (2004).
[12] V. P. Kesan, F. K. LeGoues, and S. S. Iyer, Phys. Rev. B **46**, 1576 (1992).
[13] H. Kim, H. Li, and J. M. Seo, Surf. Sci. **602**, 2563 (2008).
[14] S. Cho and J. M. Seo, J. Korean Phys. Soc. **49**, 181 (2006).
[15] G. Duvjir, H. Kim, S. M. Lee, H. Li, O. Dugerjav, S. Cho, V. C. Chu, J.-K. Lee, and J. M. Seo, Surf. Sci. **603**, 2312 (2009).
[16] Md. Zakir Hossain, H. S. Kato, and M. Kawai, Phys. Rev. B **73**, 235347 (2006).
[17] H. Nörenberg and G. A. D. Briggs, Surf. Sci. **430**, 154 (1999).
[18] K. Miki, K. Sakamoto, and T. Sakamoto, Appl. Phys. Lett. **71**, 3266 (1997).
[19] R. Butz and H. Lüth, Surf. Sci. **411**, 61 (1998).
[20] O. Leifeld, D. Grützmacher, B. Müller, K. Kern, E. Kaxiras, and P. C. Kelires, Phys. Rev. Lett. **82**, 972 (1999).
[21] S. T. Jemander, H. M. Zhang, R. I. G. Uhrberg, and G. V. Hansson, Phys. Rev. B **65**, 115321 (2002).
[22] V. De Renzi, R. Biagi, and U. del Pennino, Phys. Rev. B **64**, 155305 (2001).
[23] H. Kim, W. Kim, G. Lee, and J.-Y. Koo, Phys. Rev. Lett. **94**, 076102 (2005).
[24] T. Takaoka, T. Takagaki, Y. Igari, and I. Kusunoki, Surf. Sci. **347**, 105 (1996).
[25] R. Kosugi, S. Sumitani, T. Abukawa, S. Suzuki, S. Sato, and S. Kono, Surf. Sci. **412-413**, 125 (1998).
[26] M. L. Shek, Surf. Sci. **414**, 353 (1998).
[27] L. Simon, M. Stoffel, P. Sonnet, L. Kubler, L. Stauffer, A. Selloni, A. De Vita, R. Car, C. Pirri, G. Garreau, D. Aubel, and J. L. Bischoff, Phys. Rev. B **64**, 035306 (2001).
[28] L. Li, C. Tindall, O. Takaoka, Y. Hasegawa, and T. Sakurai, Phys. Rev. B **56**, 4648 (1997).
[29] J. R. Ahn, H. S. Lee, Y. K. Kim, and H. W. Yeom, Phys. Rev. B **69**, 233306 (2004).
[30] *User's Guide To Autoprobe VP* (Park Scientific Instruments, Sunnyvale, CA, 1996), Chap. 4.
[31] Y.-Z. Zhu, H. Kim, and J. M. Seo, Phys. Rev. B **73**, 245319 (2006).
[32] J. Knall, J. B. Pethica, J. D. Todd, and J. H. Wilson, Phys. Rev. Lett. **66**, 1733 (1991).
[33] H. Kim, H. Li, Y.-Z. Zhu, J. R. Hahn, and J. M. Seo, Surf. Sci. **601**, 1831 (2007).
[34] H. Kim, Y. Cho, and J. M. Seo, Surf. Sci. **583**, 265 (2005).
[35] H. Kim, H. Li, and J. M. Seoa, J. Vac. Sci. Technol. B **25**, 1511 (2007).
[36] Z. Gai, R. G. Zhao, W. Li, Y. Fujikawa, T. Sakurai, and W. S. Yang, Phys. Rev. B **64**, 125201 (2001).
[37] A. A. Baski and L. J. Whitman, J. Vac. Sci. Technol. B **14**, 992 (1996).
[38] F. C. Chuang, C. V. Ciobanu, C.-Z. Wang, and K.-M. Ho, J. Appl. Phys. **98**, 073507 (2005).
[39] W. Kim, H. Kim, G. Lee, and J.-Y. Koo, Phys. Rev. Lett. **89**, 106102 (2002).
[40] H. J. Osten, M. Methfessel, G. Lippert, and H. Rücker, Phys.

Rev. B **52**, 12179 (1995).
[41] J. W. Kim, T. U. Kampen, K. Horn, and M.-C. Jung, Surf. Sci. **601**, 694 (2007).
[42] C. C. Hwang, H. S. Kim, Y. K. Kim, J. S. Kim, C. Y. Park, K. J. Kim, T.-H. Kang, and B. Kim, Phys. Rev. B **59**, 14864 (1999).
[43] E. Landemark, C. J. Karlsson, Y.-C. Chao, and R. I. G. Uhrberg, Phys. Rev. Lett. **69**, 1588 (1992).
[44] F. Rochet, F. Jolly, F. Bournel, G. Dufour, F. Sirotti, and J.-L. Cantin, Phys. Rev. B **58**, 11029 (1998).